SCIENCE CHINA
Information Sciences

• RESEARCH PAPER •

January 2019, Vol. 62 012206:1–012206:16
https://doi.org/10.1007/s11432-017-9389-9

Extended state observer-based third-order sliding mode finite-time attitude tracking controller for rigid spacecraft

Chutiphon PUKDEBOON

Department of Mathematics, Faculty of Applied Science, King Mongkut's University of Technology North Bangkok, Bangkok 10800, *Thailand*

Received 7 November 2017/Revised 16 January 2018/Accepted 5 March 2018/Published online 17 October 2018

Abstract In this paper, the attitude tracking control problem for a rigid spacecraft in the presence of system parameter uncertainties and external disturbances is addressed. First, a new nonsingular finite-time sliding surface is introduced and third-order sliding mode finite-time attitude control law is designed to achieve precise accurate tracking responses and robustness against inertia uncertainties and external disturbances. The stability of the closed-loop system is rigorously proved using the Lyapunov stability theory. Then, a new finite-time extended state observer is established to estimate total disturbances of the system. The extended stated observer-based sliding mode control technique yields improved disturbance rejection and high-precision attitude tracking. Moreover, this control law can avoid the unwinding phenomenon and overcome the input saturation constraint by introducing an auxiliary variable to compensate for the overshooting. A Lyapunov based analysis is provided to guarantee sufficiently small observation error and stabilization of the closed-loop system in finite time. Numerical simulations are conducted to verify the effectiveness of the proposed control method.

Keywords third-order sliding mode, sliding mode control, extended stated observer, finite-time convergence, unwinding phenomenon

Citation Pukdeboon C. Extended state observer-based third-order sliding mode finite-time attitude tracking controller for rigid spacecraft. Sci China Inf Sci, 2019, 62(1): 012206, https://doi.org/10.1007/s11432-017-9389-9

1 Introduction

Attitude control of spacecraft has attracted much interest among researchers over past decades. The interest is motivated by its main role in many space missions such as satellite surveillance and formation flying. Because the dynamics of spacecraft are nonlinear, highly coupled and affected by various disturbances coming from the environment, an attitude controller design is usually difficult. Thus, the attitude controller designs of spacecraft are very challenging and interesting mathematical problems of great practical importance.

Various nonlinear control schemes have been proposed to address the attitude tracking control problem such as adaptive attitude control [1, 2], sliding mode control [3, 4], optimal control [5, 6], output feedback control [7], LMI-based control [8], backstepping control [9, 10], passivity-based control [11], and fuzzy control [12]. Among these methods, sliding mode control (SMC) has been widely used owing to its competence for a system with model uncertainties and external disturbances [13]. However, all results

Email: chutiphon.p@sci.kmutnb.ac.th

proposed above only ensure asymptotic stability and convergence in infinite time. The ability of control methods to provide rapid maneuver performance is highly desirable in many space missions.

Recently, terminal sliding mode control (TSMC) methods using nonlinear sliding surfaces instead of a linear surface were proposed to obtain convergence of system states in finite time [14,15]. TSMC has been given by [16, 17] for the attitude tracking of a rigid spacecraft. However, a main disadvantage of TSM control is the singularity problem. To solve this problem, the nonsingular terminal sliding mode control (NTSMC) [18, 19], nonsingular fast terminal sliding mode control (NFTSMC) [20], time-varying sliding mode [21], and integral sliding mode control (ISMC) [22, 23] have been designed to solve the attitude tracking problem.

All the results mentioned in the above literature have been derived without considering the saturation input. In practice, when the requested control torque is higher than the maximum value that the actuator can produce, a performance degradation or system instability may occur [24]. In order to overcome this drawback, several attitude control approaches with control input saturation have been increasingly taken into consideration. Wallsgrove and Akella [25] designed a saturated attitude controller by using the hyperbolic tangent function to prevent actuator saturations, while Boškovic et al. [26] used saturation functions to design saturated attitude controllers. Hu et al. [27] proposed a method of disturbance observer based finite-time attitude control design which takes actuator saturation into consideration.

To further enhance the performance of SMC, higher order sliding mode control (HOSMC) has been developed. The benefit of HOSMC is that it can reduce the chattering while still maintain the disturbance attenuation ability of SMC. Wide real-life applications have been controlled in a practical implementation of HOSMC (e.g., electropneumatic actuator [28], electric power system [29], reusable launch vehicle [30], and hybrid vehicle [31]). Second order sliding mode control (SOSMC) has widely been implemented to control many practical nonlinear systems [32–34]. In [35], an SOSMC technique has been applied to an aircraft pitch control system. In [36], a smooth SOSMC law for a missile guidance system has been developed. A SOSMC law for spacecraft attitude tracking has been developed in [22]. Finite time convergence is ensured the Lyapunov theory and homogeneity approach. An output feedback SOSMC scheme that yields chattering attenuation and finite-time stability have been proposed in [37] to deal with the attitude tracking control problem of a rigid spacecraft. Pukdeboon and his colleagues [38] have designed SOSMC and third-order sliding mode control (TOSMC) schemes for attitude tracking control of spacecraft. However, in that work, both control techniques cannot enforce finite-time convergence of the spacecraft system. Due to the difficulty of proving the finite-time stability, TOSMC designs for nonlinear spacecraft systems have been rarely studied. The main benefits of TOSMC are that it yields high accurate outputs and chattering attenuation. Therefore, the TOSMC scheme is a good choice to apply to develop an attitude tracking controller for a rigid spacecraft.

Recently, disturbance observer (DO) methods have been introduced to compensate for strong nonlinearity, unmodeled dynamics and external disturbances of uncertain systems. Among these disturbance observers, extended state observer (ESO) is widely employed in various control engineering systems such as an autonomous underwater vehicle [39] and permanent-magnet synchronous motors [40]. To further alleviate the chattering in SMC, the combination between sliding mode control and extended state observer is proposed. In [41], a missile guidance law has been presented by using an ESO. In [2, 42], ESO-based SMC methods are proposed to deal with an attitude tracking control problem of rigid spacecraft. In [43], SMC and disturbance observer are applied to systems with mismatched uncertainties. Yang et al. [44] developed a continuous nonsingular terminal sliding mode controller for systems with mismatched disturbances. In [45], dynamic SMC and higher-order mismatched disturbance observer are merged to designed a robust controller for motion control systems. Various disturbance observer designs for permanent-magnet synchronous motor (PMSM) drives are proposed in [46]. However, these control schemes study the first-order SMC design which usually provides lower performance when compared with HOSMC.

In this paper, the finite time attitude tracking control for a rigid spacecraft is examined by combing a nonsingular sliding mode control with an ESO. The ESO is designed to estimate the total disturbance. To the best knowledge of the author, there are no application of the ESO-based SMC technique to the

solution for attitude tracking of spacecraft without unwinding. Then, both adequately small observation error and stabilization of the closed-loop system are analyzed in finite time.

The main contributions of this paper are:

(1) The main feature of this controller is that it avoids the use of the first and second time derivatives of the sliding variables. These time derivatives are required in the standard TOSMC design. This is very significant because the use of time derivatives often induces the noise introduced in the controller. Moreover, the proposed control scheme is designed based on continuous TOSMC, so it is a very effective control method to deal with the chattering problem.

(2) A new structure of TOSMC is introduced in this paper. The main limitation of the exist TOSMC schemes is that the fractional power terms must be selected such that the closed-loop system is in a homogeneous form. Then, the homogeneous approach is used to prove the finite time stability. Unlike these TOSMC methods, the fractional power terms used in our proposed control approach can be selected freely. In this paper, an appropriate Lyapunov function that has state variables with an unknown fractional power is used to prove the finite-time stability of the non-homogeneous closed-loop system.

The paper is organized as follows. Section 2 describes spacecraft attitude dynamics and kinematics given by [47,48]. The problem formulation is also provided. The proposed SMC scheme with a nonsingular sliding surface for a spacecraft attitude control system is designed in Section 3. In Section 4, a new ESO is established such that the observer error dynamics converge to a bounded region containing the origin in finite time. In Section 5, simulation results are presented to show the performance of the proposed control method. In Section 6, we present the conclusion.

2 Nonlinear model and problem formulation

2.1 Spacecraft attitude dynamics and kinematics

The unit quaternion is widely used to represent the attitude kinematics of rigid spacecraft owing to its non-trigonometric expression and non-singular computations [49]. The attitude control system of a rigid spacecraft consists of kinematic and dynamic equations which can be modeled as [48]

$$\dot{q} = \frac{1}{2}(q_4 I_3 + q^{\times})\omega, \tag{1}$$

$$\dot{q}_4 = -\frac{1}{2}q^{\mathrm{T}}\omega, \tag{2}$$

$$J\dot{\omega} = -\omega^{\times}J\omega + u + d, \tag{3}$$

where $\bar{Q} = [q^{\mathrm{T}}\ q_4]^{\mathrm{T}} \in \mathbb{R}^3 \times \mathbb{R}$ is the unit quaternion vector consisting of the vector part $q \in \mathbb{R}^3$ and the scalar part q_4. They are subject to the constraint $q^{\mathrm{T}}q + q_4^2 = 1$. $J \in \mathbb{R}^{3\times 3}$ denotes the symmetric inertia matrix of the spacecraft, $\omega \in \mathbb{R}^3$ is the angular velocity of the spacecraft, $u \in \mathbb{R}^3$ represents the control vector, and $d \in \mathbb{R}^3$ are external unknown disturbances. I_3 is the 3×3 identity matrix, and for any vector $a \in \mathbb{R}^3$, a skew-symmetric matrix $a^{\times}$ is defined by

$$a^{\times} = \begin{bmatrix} 0 & -a_3 & a_2 \\ a_3 & 0 & -a_1 \\ -a_2 & a_1 & 0 \end{bmatrix}.$$

2.2 Relative attitude error dynamics and kinematics

Now the kinematic equation (1) is considered. Let the desired attitude of the spacecraft be $Q_d = [q_d^{\mathrm{T}}\ q_{4d}]^{\mathrm{T}} \in \mathbb{R}^3 \times \mathbb{R}$ where $q_d \in \mathbb{R}^3$, $q_{4d} \in \mathbb{R}$, and ω_d be the desired angular velocity. Then, the desired attitude motion is generated by

$$\dot{q}_d = \frac{1}{2}(q_{4d} I_3 + q_d^{\times})\omega_d, \tag{4}$$

$$\dot{q}_{4d} = -\frac{1}{2} q_d^{\mathrm{T}} \omega_d. \tag{5}$$

The quaternion error $Q_e = [q_e^{\mathrm{T}} \ q_{4e}]^{\mathrm{T}} \in \mathbb{R}^3 \times \mathbb{R}$ represents the relative attitude error from the body-fixed reference frame to the desired reference frame. Using the quaternion multiplication law, the quaternion error [49] is obtained as

$$Q_e = \begin{bmatrix} q_{4d} q - q_4 q_d - q_d^{\times} q \\ q_4 q_{4d} + q^{\mathrm{T}} q_d \end{bmatrix} \tag{6}$$

satisfying the constraint

$$Q_e^{\mathrm{T}} Q_e = (q^{\mathrm{T}} q + q_4^2)(q_d^{\mathrm{T}} q_d + q_{4d}^2) = 1. \tag{7}$$

As a result, the relative attitude error can be expressed as [42]

$$\begin{aligned} \dot{q}_e &= \frac{1}{2} T(Q_e) \omega_e, \\ \dot{q}_{4e} &= -\frac{1}{2} q_e^{\mathrm{T}} \omega_e, \end{aligned} \tag{8}$$

where $T(Q_e) = q_e^{\times} + q_{4e} I_3$.

Define the angular velocity error as $\omega_e = \omega - C\omega_d$, where C denotes the rotation matrix given by $C = (q_{4e}^2 - 2q_e^{\mathrm{T}} q_e) I_3 + 2 q_e q_e^{\mathrm{T}} - 2 q_{4e} q_e^{\times}$. Note that $\|C\| = 1$ and $\dot{C} = -\omega_e^{\times} C$. The first time derivative of ω_e is

$$\dot{\omega}_e = \dot{\omega} + \omega_e^{\times} C \omega_d - C \dot{\omega}_d. \tag{9}$$

Substituting (9) into (3), the dynamic equation of the error rate can be written as

$$\begin{aligned} J\dot{\omega}_e &= -(\omega_e + \omega_r)^{\times} J(\omega_e + \omega_r) + u + d + J(\omega_e^{\times} C\omega_d - C\dot{\omega}_d) \\ &= -\omega^{\times} J\omega + J(\omega_e^{\times} C\omega_d - C\dot{\omega}_d) + u + d. \end{aligned} \tag{10}$$

To consider the inertia uncertainties of the spacecraft system, Assumption 1 is required.

Assumption 1. The inertia matrix in (3) can be described as $J = J_0 + \Delta J$ where J_0 is the known nonsingular constant matrix and ΔJ denotes the uncertain inertia matrix.

Letting $\omega_r = C\omega_d$ and substituting $J = J_0 + \Delta J$ into (10), the spacecraft attitude dynamics (10) can be rewritten as

$$J_0 \dot{\omega}_e = -\omega^{\times} J_0 \omega - J_0 \dot{\omega}_r + u + \tilde{d}, \tag{11}$$

where $\dot{\omega}_r = C\dot{\omega}_d - \omega_e^{\times} C\omega_d$ and $\tilde{d} = d - \Delta J \dot{\omega} - \omega^{\times} \Delta J \omega$.

Before describing the controller design in later sections, Assumption 2 is needed.

Assumption 2. Assume that the total uncertainty vector $\tilde{d} \in \mathcal{C}^2$ and satisfies $\|\ddot{\tilde{d}}\| \leqslant \bar{\psi}$, where $\bar{\psi}$ is a positive constant.

Remark 1. The unknown external disturbance includes environmental disturbance, solar radiation and magnetic effects. These factors are all bounded and continuous in practice. The desired angular velocity and its first time derivative are assumed to be bounded and differentiable. Moreover, the control inputs are restricted with maximum torques produced by generating devices, so the state variables are normally bounded and differentiable. Therefore, it is reasonable to suppose that the total disturbance and its higher order are bounded as given in Assumption 2. The boundedness condition is a common requirement in many existing spacecraft attitude control results [50–52].

2.3 Problem statement

In this paper, we assume that the quaternion and angular velocity measurements are always available. Also, the desired angular velocity ω_d and its first time derivative $\dot{\omega}_d$ are bounded. The main control objective is to developed an ESO-based TOSMC approach such that the attitude and angular velocity errors converge to a small neighborhood about zero in finite time. This can be expressed as

$$\lim_{t \to T} (q_e(t), \omega_e(t)) \in \Omega_c, \tag{12}$$

where T is a finite time and Ω_c denotes a small region containing the origin.

3 Unwinding finite-time attitude control via TOSMC

The main purpose of this section is to present a TOSMC controller design to solve the finite-time attitude tracking control problem. Using Lyapunov theory analysis, the proposed controller ensures that attitude tracking and angular velocity errors converge to a desired region in finite time.

Now, we define the auxiliary variable as

$$z = \omega_e + K\text{sign}(q_{4e})q_e, \tag{13}$$

where $K > 0$ is a diagonal matrix. The first time derivative of z can be obtained as

$$\dot{z} = -J_0^{-1}\omega^{\times}J_0\omega - \dot{\omega}_r + J_0^{-1}u + J_0^{-1}\tilde{d} + \frac{1}{2}K\text{sign}(q_{4e})T(Q_e)\omega_e. \tag{14}$$

Now, we define the sliding surface as

$$s_i = z_i + \int_0^t \phi \mathrm{d}\tau, \tag{15}$$

where ϕ is defined as

$$\phi_i = c_{1i}|z_i|^{1+\frac{1}{\gamma}}\text{sign}(z_i) + c_{2i}e^{\lambda|z_i|}z_i + c_{3i}|z_i|^{1-\frac{1}{\gamma}}\text{sign}(z_i), \tag{16}$$

where $\gamma > 1$, c_{1i}, c_{2i} and c_{3i}, $i = 1, 2, 3$ are positive constants satisfying $4c_{1i}c_{3i} > c_{2i}^2$. In (16), e is the Euler number and λ is a positive constant. Therefore, the dynamics of the associate sliding mode can be obtained as

$$\dot{z}_i = -c_{1i}|z_i|^{1+\frac{1}{\gamma}}\text{sign}(z_i) - c_{2i}e^{\lambda|z_i|}z_i - c_{3i}|z_i|^{1-\frac{1}{\gamma}}\text{sign}(z_i), \quad (i = 1, 2, 3). \tag{17}$$

We now show that the states $z_i = 0$ $(i = 1, 2, 3)$ of the dynamics (17) converge to zero in finite time.

Theorem 1. The zero solution $z_i = 0$ $(i = 1, 2, 3)$, of the sliding mode dynamics (17) is globally fixed-time stable and the settling time is given by

$$T \leqslant \frac{2\gamma}{\sqrt{4c_{1i}c_{3i} - c_{2i}^2}}\left(\frac{\pi}{2} - \arctan\left(\frac{c_{2i}}{\sqrt{4c_{1i}c_{3i} - c_{2i}^2}}\right)\right). \tag{18}$$

Proof. The Lyapunov function candidate is chosen as

$$V_1 = |z_i|. \tag{19}$$

Its first time derivative is

$$\begin{aligned}\dot{V}_1 &= \text{sign}(z_i)\dot{z}_i \\ &= \text{sign}(z_i)\left(-c_{1i}|z_i|^{1+\frac{1}{\gamma}}\text{sign}(z_i) - c_{2i}e^{\lambda|z_i|}z_i - c_{3i}|z_i|^{1-\frac{1}{\gamma}}\text{sign}(z_i)\right) \\ &= -c_{1i}|z_i|^{1+\frac{1}{\gamma}} - c_{2i}e^{\lambda|z_i|}z_i - c_{3i}|z_i|^{1-\frac{1}{\gamma}}.\end{aligned} \tag{20}$$

For $\alpha > 0$, one has $e^{(\alpha|z_i|)} > e^0 = 1$ and it follows that

$$\begin{aligned}\dot{V}_1 &\leqslant -c_{1i}|z_i|^{1+\frac{1}{\gamma}} - c_{2i}z_i - c_{3i}|z_i|^{1-\frac{1}{\gamma}} \\ &\leqslant -c_{1i}V_1^{1+\frac{1}{\gamma}} - c_{2i}V_1 - c_{3i}V_1^{1-\frac{1}{\gamma}}.\end{aligned} \tag{21}$$

It follows that

$$\begin{aligned}\mathrm{d}t &\leqslant \frac{-\mathrm{d}V_1}{c_{1i}V_1^{1+\frac{1}{\gamma}} + c_{2i}V_1 + c_{3i}V_1^{1-\frac{1}{\gamma}}} \\ &\leqslant \frac{-\mathrm{d}V_1^{\frac{1}{\gamma}}}{V_1^{\frac{1}{\gamma}-1}(c_{1i}V_1^{1+\frac{1}{\gamma}} + c_{2i}V_1 + c_{3i}V_1^{1-\frac{1}{\gamma}})}.\end{aligned} \tag{22}$$

Let $\varpi = V_1^{\frac{1}{\gamma}}$, and then $\mathrm{d}\varpi = \frac{1}{\gamma} V_1^{1-\frac{1}{\gamma}} \mathrm{d}V_1$. Thus, Eq. (22) becomes

$$\begin{aligned} \mathrm{d}t &\leqslant \frac{-\gamma \mathrm{d}\varpi}{c_{1i}\varpi^2 + c_{2i}\varpi + c_{3i}} \\ &\leqslant \frac{-\gamma \mathrm{d}\varpi}{c_{1i}\left((\varpi + \frac{c_{2i}}{2c_{1i}})^2 + \left(\frac{\sqrt{4c_{1i}c_{3i} - c_{2i}^2}}{2c_{1i}}\right)^2\right)}. \end{aligned} \tag{23}$$

Taking the integral of both sides from 0 to T and letting $V_1(T)$, one obtains

$$T \leqslant \frac{2\gamma}{\sqrt{4c_{1i}c_{3i} - c_{2i}^2}} \left(\arctan\left(\frac{2c_{1i}V_1^{\frac{1}{\gamma}}(0) + c_{2i}}{\sqrt{4c_{1i}c_{3i} - c_{2i}^2}} \right) - \arctan\left(\frac{c_{2i}}{\sqrt{4c_{1i}c_{3i} - c_{2i}^2}} \right) \right). \tag{24}$$

Obviously, T is bounded by a constant defined by (20). By the concept of fixed-time stability, it can conclude that $z_i = 0 \ \ (i = 1, 2, 3)$ are fixed-time stabilized. This completes the proof.

We now consider the spacecraft systems (8) and (11) in the presence of the disturbance $\tilde{d}(t)$. The proposed control law is designed as

$$u(t) = u_{eq}(t) + u_s(t), \tag{25}$$

where

$$u_{eq} = \omega^{\times} J_0 \omega + J_0 \dot{\omega}_r - J_0 K \mathrm{sign}(q_{4e})(q_{4e} I_3 + q_e^{\times})\omega_e - C_1 \mathrm{sign}^{1+\frac{1}{\gamma}}(s) - C_2 \mathrm{sign}^{1-\frac{1}{\gamma}}(s) \tag{26}$$

with $\gamma \in (0, 1)$ and

$$u_s(t) = -J_0\beta_1 \mathrm{sign}^{\rho}(s) - J_0\beta_2 \int_0^t \mathrm{sign}^{\rho}(s(\tau))\mathrm{d}\tau - J_0\beta_3 \int_0^t \int_0^{\tau} \mathrm{sign}^{2\rho-1}(s(\upsilon))\mathrm{d}\upsilon\mathrm{d}\tau \tag{27}$$

with $\rho \in (0.5, 1)$. In (26) and (27) for $\alpha \in (0, 1)$, the function $\mathrm{sign}^{\alpha}(s)$ is defined as

$$\mathrm{sign}^{\alpha}(s) = \begin{bmatrix} |s_1|^{\alpha}\mathrm{sign}(s_1) \\ |s_2|^{\alpha}\mathrm{sign}(s_2) \\ |s_3|^{\alpha}\mathrm{sign}(s_3) \end{bmatrix}.$$

Next, the convergence of the system state errors to the origin is analyzed in Theorem 2.

Theorem 2. Consider the spacecraft system in the presence of the disturbance $\tilde{d}(t)$. If the proposed controller is defined by (25), then the sliding surface $s(t)$ can be stabilized to a neighborhood of zero in finite time.

Proof. Differentiating (14) with respect to time and then premultiplying the results by J_0, one can obtain

$$J_0\dot{s}(t) = -\omega^{\times} J_0 \omega - J_0 \dot{\omega}_r + \frac{1}{2} J_0 K \mathrm{sign}(q_{4e}) T(Q_e)\omega_e + C_1 \mathrm{sign}^{1+\frac{1}{\gamma}}(s) + C_2 \mathrm{sign}^{1-\frac{1}{\gamma}}(s) + u + \tilde{d}. \tag{28}$$

Substituting the control law (25) into (28), one gains

$$\dot{s} = -\beta_1 \mathrm{sign}^{\rho}(s) - \beta_2 \int_0^t \mathrm{sign}^{\rho}(s(\tau))\mathrm{d}\tau - \beta_3 \int_0^t \int_0^{\tau} \mathrm{sign}^{2\rho-1}(s(\upsilon))\mathrm{d}\upsilon\mathrm{d}\tau. \tag{29}$$

Let

$$\phi_1 = -\beta_2 \int_0^t \mathrm{sign}^{\rho}(s(\tau))\mathrm{d}\tau + \tilde{d}(t) - \beta_3 \int_0^t \int_0^{\tau} \mathrm{sign}^{2\rho-1}(s(\upsilon))\mathrm{d}\upsilon\mathrm{d}\tau, \tag{30}$$

and

$$\phi_2 = -\beta_3 \int_0^t \mathrm{sign}^{2\rho-1}(s(\tau))\mathrm{d}\tau + \dot{\tilde{d}}(t). \tag{31}$$

Setting $z_1 = s$, $z_2 = \phi_1$, $z_3 = \phi_2$ and $\psi(t) = \ddot{\tilde{d}}(t)$, then (29) can be rewritten as in the scalar form $(i = 1, 2, 3)$ as

$$\begin{aligned}
\dot{z}_{1i} &= -\beta_{1i}|z_{1i}|^{\rho}\text{sign}(z_{1i}) + z_{2i},\\
\dot{z}_{2i} &= -\beta_{2i}|z_{1i}|^{\rho}\text{sign}(z_{1i}) + z_{3i},\\
\dot{z}_{3i} &= -\beta_{3i}|z_{1i}|^{2\rho-1}\text{sign}(z_{1i}) + \psi(t).
\end{aligned} \tag{32}$$

Next, it requires to ensure that the states z_{1i}, z_{2i} and z_{3i} $(i = 1, 2, 3)$ converge to the neighborhood of zero in finite time. The Lyapunov function is selected as

$$V_2(t) = \vartheta^{\mathrm{T}} P \vartheta, \tag{33}$$

where $\vartheta = [|z_{1i}|^{\rho}\text{sign}(z_{1i})\ z_{2i}\ z_{3i}]^{\mathrm{T}}$ and

$$P = \begin{bmatrix} \dfrac{\beta_{1i}}{\rho} + \beta_{2i}^2 + \beta_{3i}^2 & -\beta_{2i} & -\beta_{3i} \\ -\beta_{2i} & 2 & 0 \\ -\beta_{3i} & 0 & 2 \end{bmatrix}. \tag{34}$$

Note that V_2 satisfies

$$\lambda_{\min}(P)\|\vartheta\|^2 \leqslant V_2 \leqslant \lambda_{\max}(P)\|\vartheta\|^2, \tag{35}$$

and $\lambda_{\min}(P)$ and $\lambda_{\max}(P)$ are the minimum and maximum singular values of the matrix P.

The first time derivative of $\vartheta(t)$ is obtained as

$$\dot{\vartheta}(t) = \begin{bmatrix} \rho|z_{1i}|^{\rho-1}\left(z_{2i} - \beta_{1i}\text{sign}^{\rho}(z_{1i})\right) \\ z_{3i} - \beta_{2i}\text{sign}^{\rho}(z_{1i}) \\ -\beta_{3i}\text{sign}^{2\rho-1}(z_{1i}) + \psi(t) \end{bmatrix} = A\vartheta + B\psi(t), \tag{36}$$

where

$$A = \begin{bmatrix} -\rho\alpha\beta_{1i} & -\rho\alpha & 0 \\ -\beta_{2i} & 0 & 1 \\ -\alpha\beta_{3i} & 0 & 0 \end{bmatrix} \quad \text{and} \quad B = \begin{bmatrix} 0 \\ 0 \\ 1 \end{bmatrix}, \tag{37}$$

where $\alpha = |z_{1i}|^{\rho-1} > 0$. The characteristic equation of the matrix A is obtained as

$$G(\tilde{s}) = \tilde{s}^3 + \rho\alpha\beta_{1i}\tilde{s}^2 + \rho\alpha\beta_{2i}\tilde{s} + \rho\alpha^2\beta_{3i}. \tag{38}$$

If there exist β_{1i}, β_{2i}, $\beta_{3i} > 0$ and $z_{1i} \neq 0$, then $G(\tilde{s})$ is Hurwitz which implies that the matrix A is stable. The time derivative of $V_2(\vartheta(t))$ is

$$\begin{aligned}
\dot{V}_2(t) &= \dot{\vartheta}^{\mathrm{T}} P \vartheta + \vartheta^{\mathrm{T}} P \dot{\vartheta} \\
&= \left(A\vartheta + B\psi(t)\right)^{\mathrm{T}} P\vartheta + \vartheta^{\mathrm{T}} P\left(A\vartheta + B\psi(t)\right) \\
&= \vartheta^{\mathrm{T}}\left(A^{\mathrm{T}}P + PA\right)\vartheta + 2\bar{\psi}\hat{B}^{\mathrm{T}}\vartheta,
\end{aligned} \tag{39}$$

where $\hat{B}^{\mathrm{T}} = B^{\mathrm{T}}P = [-\beta_{3i}\ 0\ 2]$ and $\bar{\psi} = \max(|\psi_i(t)|)$, $i = 1, 2, 3$. Since A is a Hurwitz matrix, there is a positive definite matrix Q such that

$$A^{\mathrm{T}}P + PA = -Q. \tag{40}$$

Considering $\|\vartheta\|^2 = |z_{1i}| + z_{2i}^2 + z_{3i}^2$, it follows that

$$\|\vartheta\| \geqslant |z_{1i}|^{\frac{1}{2}}. \tag{41}$$

Using (40) and (41), the inequality is obtained as

$$\dot{V}_2(t) = -\vartheta^{\mathrm{T}} Q \vartheta + 2\bar{\psi}\hat{B}^{\mathrm{T}}\vartheta$$

$$\begin{aligned}&\leqslant -\lambda_{\min}(Q)\|\vartheta\|^2 + 2\bar{\psi}\|\hat{B}\|\|\vartheta\|\\&= -\left(\lambda_{\min}(Q)\|\vartheta\| - 2\bar{\psi}\|\hat{B}\|\right)\|\vartheta\|.\end{aligned} \tag{42}$$

The matrix A can be expressed as

$$-A = A_1 A_2, \tag{43}$$

where

$$A_1 = \begin{bmatrix}\rho\alpha & 0 & 0\\ 0 & 1 & 0\\ 0 & 0 & \alpha\end{bmatrix} \quad \text{and} \quad A_2 = \begin{bmatrix}\beta_{1i} & -1 & 0\\ \beta_{2i} & 0 & -1\\ \beta_{3i} & 0 & 0\end{bmatrix}. \tag{44}$$

It follows that

$$\lambda_{\min}(A_1)\lambda_{\min}(A_2) \leqslant \lambda_{\min}(A_1 A_2) = \lambda_{\min}(-A). \tag{45}$$

Since A is a diagonal matrix and $\rho\alpha < \alpha$, there exists

$$\lambda_{\min}(A_1) = \begin{cases}1, & |z_{1i}| < \left(\dfrac{1}{\rho}\right)^{\frac{1}{\rho-1}},\\ \rho\alpha, & |z_{1i}| \geqslant \left(\dfrac{1}{\rho}\right)^{\frac{1}{\rho-1}}.\end{cases}$$

If $|z_{1i}| \geqslant (\frac{1}{\rho})^{\frac{1}{\rho-1}}$ then $\|\vartheta\| \geqslant (\frac{1}{\rho})^{\frac{\rho}{\rho-1}}$. One can have

$$\lambda_{\min}(Q) \geqslant 2\rho\alpha\lambda_{\min}(A_2)\lambda_{\min}(P). \tag{46}$$

Considering (42) and (46), one has

$$\begin{aligned}\delta_1 &= \lambda_{\min}(Q)\|\vartheta\| - 2\|\hat{B}\|\bar{\psi}\\&\geqslant 2\alpha\rho\lambda_{\min}(A_2)\lambda_{\min}(P)|z_{1i}|^{\rho} - 2\|\hat{B}\|\bar{\psi}\\&= 2\rho|z_{1i}|^{\rho-1}\lambda_{\min}(A_2)\lambda_{\min}(P)|z_{1i}|^{\rho} - 2\|\hat{B}\|\bar{\psi}\\&\geqslant 2\rho\left(\frac{1}{\rho}\right)^{\frac{2\rho-1}{\rho-1}}\lambda_{\min}(A_2)\lambda_{\min}(P) - 2\|\hat{B}\|\bar{\psi}.\end{aligned} \tag{47}$$

With $\rho \in (0.5, 1)$, there exists a constant ϕ such that

$$2\rho\left(\frac{1}{\rho}\right)^{\frac{2\rho-1}{\rho-1}} \geqslant \phi. \tag{48}$$

Letting $\delta_{1m} = \phi\lambda_{\min}(A_2)\lambda_{\min}(P) - 2\|\hat{B}\|\bar{\psi} > 0$ and choosing the suitable parameters β_{1i}, β_{2i} and β_{3i} such that $\phi\lambda_{\min}(A_2)\lambda_{\min}(P) > 2\|\hat{B}\|\bar{\psi}$, one obtains

$$\dot{V}_2(t) \leqslant -\frac{\delta_{1m}}{\sqrt{\lambda_{\max}(P)}}V_2^{\frac{1}{2}} = -\Lambda_1 V_2^{\frac{1}{2}}, \tag{49}$$

where $\Lambda_1 = \frac{\delta_{1m}}{\sqrt{\lambda_{\max}(P)}}$. Based on concepts of finite-time stability given by [14], $\|\vartheta\|$ converges to the region $\|\vartheta\| \leqslant (\frac{1}{\rho})^{\frac{\rho}{\rho-1}}$ in finite time t_{s1} defined as

$$t_{s1} \leqslant \frac{2}{\Lambda_1}V_2^{\frac{1}{2}}(\vartheta(t)) \leqslant \frac{2}{\Lambda_1}V_2^{\frac{1}{2}}(\vartheta(t_0)). \tag{50}$$

If $\|\vartheta\| < (\frac{1}{\rho})^{\frac{\rho}{\rho-1}}$ then $|z_{1i}| < (\frac{1}{\rho})^{\frac{1}{\rho-1}}$. Therefore, there is

$$\lambda_{\min}(Q) \geqslant 2\lambda_{\min}(A_2)\lambda_{\min}(P). \tag{51}$$

According to (42) and (51), one obtains

$$\begin{aligned}\delta_2 &= \lambda_{\min}(Q)\|\vartheta\| - 2\|\hat{B}\|\bar{\psi} \\ &\geqslant 2\lambda_{\min}(A_2)\lambda_{\min}(P)\|\vartheta\| - 2\|\hat{B}\|\bar{\psi}. \end{aligned} \tag{52}$$

If

$$\left(\frac{1}{\rho}\right)^{\frac{\rho}{\rho-1}} > \|\vartheta\| > \frac{\|\hat{B}\|\bar{\psi}}{\lambda_{\min}(A_2)\lambda_{\min}(P)} = \Psi \tag{53}$$

is satisfied, then there exists

$$\delta_2 > 2\lambda_{\min}(A_2)\lambda_{\min}(P)\Psi - 2\|\hat{B}\|\bar{\psi} = 0. \tag{54}$$

It follows that

$$\dot{V}_2(t) \leqslant -\frac{\delta_2}{\sqrt{\lambda_{\max}(P)}} V_2^{\frac{1}{2}}(\vartheta(t)) = -\Lambda_2 V_2^{\frac{1}{2}}(\vartheta(t)), \tag{55}$$

where $\Lambda_2 = \frac{\delta_2}{\sqrt{\lambda_{\max}(P)}}$. Then, one obtains

$$t_{s2} \leqslant \frac{2}{\Lambda_2} V_2^{\frac{1}{2}}(\vartheta(t)) \leqslant \frac{2}{\Lambda_2} V_2^{\frac{1}{2}}(\vartheta(t_{s1})). \tag{56}$$

Therefore, $\|\vartheta\|$ is decreased and converges to the region

$$\|\vartheta\| \leqslant \frac{\|\hat{B}\|\bar{\psi}}{\lambda_{\min}(A_2)\lambda_{\min}(P)} \tag{57}$$

in finite time $t_s = t_{s1} + t_{s2}$.

Obviously, if the suitable parameters β_{1i}, β_{2i} and β_{3i} are chosen such that $\lambda_{\min}(A_2)\lambda_{\min}(P)$ is sufficiently large, then $\|\vartheta\|$ is limited to sufficiently small in finite time. This implies that $s_i = z_{1i}$ $(i = 1, 2, 3)$ converge to a neighborhood of zero in finite time. The proof is completed.

4 Nonlinear disturbance observer

In this section, a nonlinear disturbance observer is designed to estimate the total disturbance $\tilde{d}$. In practical engineering, the specific information of the total disturbance is difficult to obtain owing to the complicate structure of disturbance. However, it is reasonable to assume that $\tilde{d}$, $\dot{\tilde{d}}$ and $\ddot{\tilde{d}}$ are bounded.

4.1 Extended state observer

In a general way, the system (14) can be written as

$$\dot{x} = F + J_0^{-1}u + G, \tag{58}$$

where $x = z$, $F = -J_0^{-1}\omega^{\times}J_0\omega - \dot{\omega}_r + \frac{1}{2}K\text{sign}(q_{4e})T(Q_e)\omega_e$ and $G = J_0^{-1}\tilde{d}$.

We can rewrite (58) with extended states as

$$\begin{aligned}\dot{x}_1 &= F(x_1) + J_0^{-1}u + x_2, \\ \dot{x}_2 &= x_3, \\ \dot{x}_3 &= h(t), \end{aligned} \tag{59}$$

where $h(t)$ is the second time derivatives of the total disturbance G. To approximate the compounded disturbance of the system (58), the proposed extended state observer is designed as

$$\begin{aligned}\dot{Z}_1 &= Z_2 + F(x_1) + J_0^{-1}u - \lambda_1\text{sign}^{\kappa}(Z_1 - x_1), \\ \dot{Z}_2 &= Z_3 - \lambda_2\text{sign}^{\kappa}(Z_1 - x_1), \\ \dot{Z}_3 &= -\lambda_3\text{sign}^{2\kappa-1}(Z_1 - x_1), \end{aligned} \tag{60}$$

where $\kappa \in (0.5, 1)$, Z_1, Z_2 and Z_3 are the estimates of x_1, G and $\dot{G}$, respectively. The convergence proof for the proposed ESO is given in Theorem 3.

Theorem 3. Considering the proposed ESO (60) and Assumption 2, there exist observer parameters λ_{1i}, λ_{2i} and λ_{2i}, $i = 1, 2, 3$ such that the observer error states converge to a small region containing the origin in finite time.

Proof. Let $e_1 = Z_1 - x_1$, $e_2 = Z_2 - x_2$ and $e_3 = Z_3 - x_3$. From the system (59) and the designed ESO (60), the corresponding observer error dynamics can be written in the scalar form ($i = 1, 2, 3$) as

$$\begin{aligned}
\dot{e}_{1i} &= e_{2i} - \lambda_{1i}|e_{1i}|^{\kappa}\mathrm{sign}(e_{1i}),\\
\dot{e}_{2i} &= e_{3i} - \lambda_{2i}|e_{1i}|^{\kappa}\mathrm{sign}(e_{1i}),\\
\dot{e}_{3i} &= -\lambda_{3i}|e_{1i}|^{2\kappa-1}\mathrm{sign}(e_{1i}) + h(t).
\end{aligned} \tag{61}$$

Evidently, the closed-loop system (61) is the same form of the system (32) presented in Theorem 2. Thus, the stability proof can be analyzed by following the similar process in Theorem 2. This completes the proof.

Thus, the proposed ESO-based TOSMC is given by

$$u = u_{eq} + u_s - J_0 Z_2. \tag{62}$$

One can conclude that if the inertia uncertainties ΔJ and external disturbance $d(t)$ are twice differentiable. The total disturbance G can be compensated by the proposed ESO.

Remark 2. Normally, existing ESO results are based on the algorithms presented in [39–41]. These ESO schemes did not use SMC concepts. In this paper, to improve the robust performance, the new structure of ESO is introduced by employing TOSMC technique. Compared to those ESO results, our proposed ESO is more robust against noise that may occur in the observed process.

4.2 Attitude control with input saturation

In practical application, input saturation must be considered because the torques applied to the spacecraft system cannot be larger than the maximum torques generated by the actuators.

Consider the rigid spacecraft system with actuator constraints

$$J_0\dot{\omega}_e = -\omega^{\times} J_0\omega - J_0\dot{\omega}_r + \mathrm{sat}(u) + \tilde{d}, \tag{63}$$

where $\mathrm{sat}(u) = [\mathrm{sat}(u_1)\ \mathrm{sat}(u_2)\ \mathrm{sat}(u_3)]^{\mathrm{T}}$ is the saturated torque produced by the actuators (or thrusters). The saturation function $\mathrm{sat}(u_i)$, $i = 1, 2, 3$ is of the form

$$\mathrm{sat}(u_i) = \mathrm{sign}(u_i)\min(u_{\max,i}, |u_i|), \tag{64}$$

where $u_{\max,i}$ and $u_{\min,i}$, $i = 1, 2, 3$ are the maximum and minimum output torques. This saturated torque can be expressed as

$$\mathrm{sat}(u) = u + \delta u, \tag{65}$$

where δu_i is given by

$$\delta u_i = \begin{cases} u_{\max,i} - u_i, & u_i > u_{\max,i},\\ 0, & u_{\min,i} \leqslant u_i \leqslant u_{\max,i},\\ u_{\min,i} - u_i, & u_i < u_{\min,i}. \end{cases} \tag{66}$$

Substituting (65) into (63), we obtains

$$J_0\dot{\omega}_e = -\omega^{\times} J_0\omega - J_0\dot{\omega}_r + u + \delta u + \tilde{d}. \tag{67}$$

Considering the dynamic equation (11), let the total disturbance $\tilde{d}$ be defined as

$$\tilde{d} = d - \Delta J\dot{\omega} - \omega^{\times}\Delta J\omega + \delta u. \tag{68}$$

Then the stability of the closed-loop system can be analyzed by following the same steps presented in Theorem 2.

Remark 3. For a given practical system, the term δu cannot be too large. If this term is too big, it means that the actuator cannot generate sufficiently large control torques to make system stable [53]. According to the controllability of a practical system, it is reasonable that $\|\delta u\|$ is always bounded by a constant.

5 Simulations

Numerical simulations have been conducted to demonstrate the performance of the proposed ESO-based TOSMC scheme and the fast terminal sliding mode control (FTSMC) law in [20]. Consider the spacecraft system with the nominal inertia matrix

$$J = \begin{bmatrix} 20 & 1.2 & 0.9 \\ 1.2 & 17 & 1.4 \\ 0.9 & 1.4 & 15 \end{bmatrix} \quad \text{kg} \cdot \text{m}^2, \tag{69}$$

and the uncertain inertia

$$\Delta J = \text{diag}\left(\sin(0.1t), 2\sin(0.2t), 3\sin(0.3t)\right) \quad \text{kg} \cdot \text{m}^2. \tag{70}$$

Suppose that attitude control problem is considered with the periodic disturbances provided by

$$d(t) = 0.1\left[\sin(0.1t) \;\; \sin(0.2t) \;\; \sin(0.3t)\right]. \tag{71}$$

The desired angular velocity is assumed to be

$$\omega_d(t) = 0.05\left[\sin\left(\frac{\pi t}{100}\right) \;\; \sin\left(\frac{2\pi t}{100}\right) \;\; \sin\left(\frac{3\pi t}{100}\right)\right] \quad \text{rad/s}. \tag{72}$$

Numerical simulations are performed by using the initial quaternion and angular velocities chosen as $Q(0) = [-0.2 \;\; 0.4 \;\; 0.7 \;\; -0.5568]^{\mathrm{T}}$ and $\omega(0) = [-0.04 \;\; -0.12 \;\; 0.05]^{\mathrm{T}}$ rad/s. Also, the initial desired quaternion is selected as $Q_d(0) = [0 \;\; 0 \;\; 0 \;\; -1]^{\mathrm{T}}$. The limitation of output torques are $u_{\max,i} = 2.5$ and $u_{\mathrm{mim},i} = -2.5$ N-m, $i = 1, 2, 3$.

For the FTSMC in [20], the attitude tracking motion is considered with the focus on the following parameters: $k_1 = 1.5$, $k_2 = 0.1$, $\gamma = 0.8$, $\alpha = 0.7$, $\beta = 0.1$, $\lambda = 0.0005$ and $\eta = 0.00001$. On the other hand, the control parameters of the ESO-based TOSMC are selected as $K = 0.8I_3$, $\beta_1 = 5I_3$, $\beta_2 = 3I_3$, $\beta_3 = 0.2I_3$, $\rho = 0.75$, $\lambda = 1.0$, $c_{1i} = 0.2$, $c_{2i} = 0.1$ and $c_{3i} = 0.2$, $i = 1, 2, 3$. For the proposed observer (60), the parameters are chosen as $\kappa = 0.8$, $\lambda_{1i} = 5$, $\lambda_{2i} = 7$ and $\lambda_{3i} = 1$, $i = 1, 2, 3$. It should be noted that all control parameters for the ESO-based TOSMC method must be chosen such that the condition $\phi\lambda_{\min}(A_2)\lambda_{\min}(P) > 2\|\hat{B}\|\bar{\psi}$ and the simulation results are satisfied. In other words, control parameters are reassigned until the condition and satisfied simulation results are achieved.

From Figures 1(a)–(c), one can see that the proposed ESO-based TOSMC scheme achieves faster stabilization of attitude tracking errors to zero. As shown in Figure 1(d) when the ESO-based TOSMC is applied, the scalar quaternion converges to $q_{4e} = -1$ quicker than one of the FTSMC method. Both the FTSMC in [20] and proposed controller avoid the occurrence of unwinding phenomenon. Figures 2(a)–(c) show that the proposed controller is able to drive angular velocity tracking errors to zero with faster convergence rate than the FTSMC in [20]. From Figures 3(a)–(c), it can be seen that the sliding variables under the FTSMC in [20] and proposed controller approach the sliding manifold $s_i = 0$ $(i = 1, 2, 3)$ in finite time.

As shown in Figures 4(a)–(c), control signals obtained by the ESO-based TOSMC scheme have less variation when compared with the FTSMC [20]. As shown in Figures 5(a)–(c), the disturbances estimated by the proposed ESO can track the true values in finite time. In the final steady state, the tracking errors of FTSMC are $\|q_e\| \leqslant 2.81 \times 10^{-5}$ and $\|\omega_e\| \leqslant 2.93 \times 10^{-5}$ and $\|s\| \leqslant 3.54 \times 10^{-5}$ with sampling time $h = 0.005$. On the other hand, the steady state tracking accuracy attained by the ESO-based TOSMC

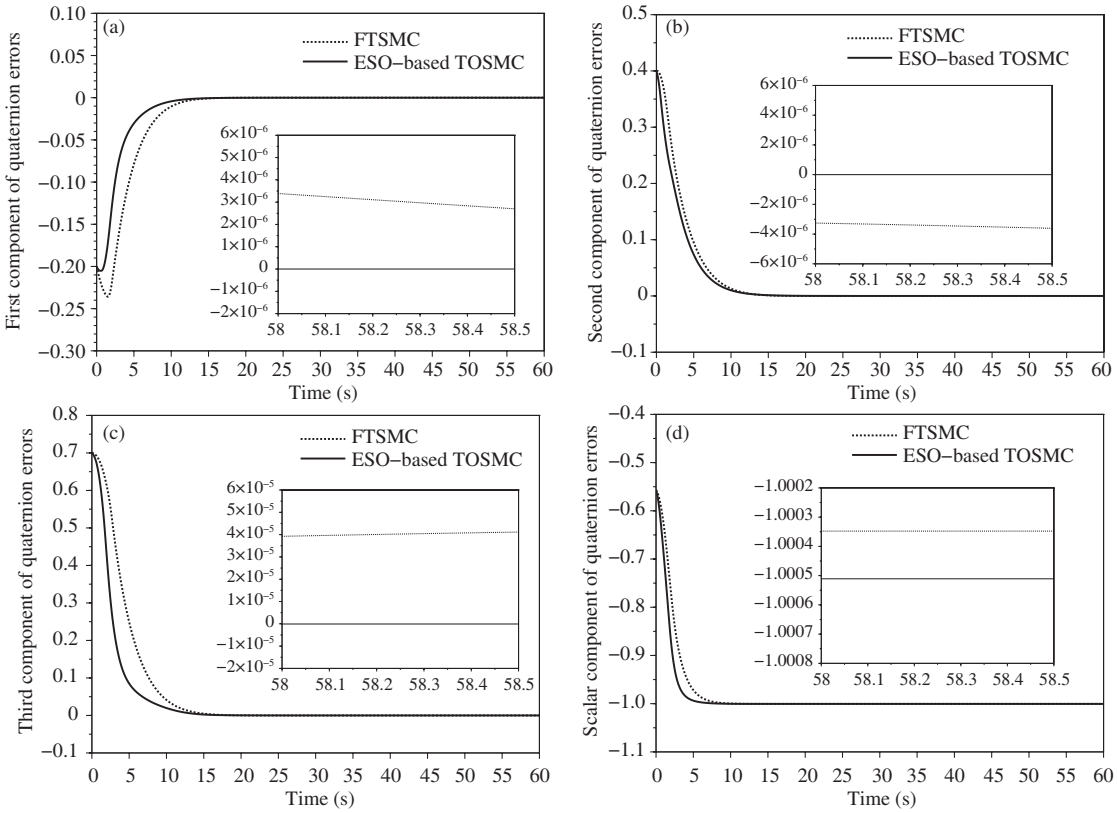

Figure 1 Attitude tracking error responses. The time history of (a) q_{1e}, (b) q_{2e}, (c) q_{3e}, (d) q_{4e}.

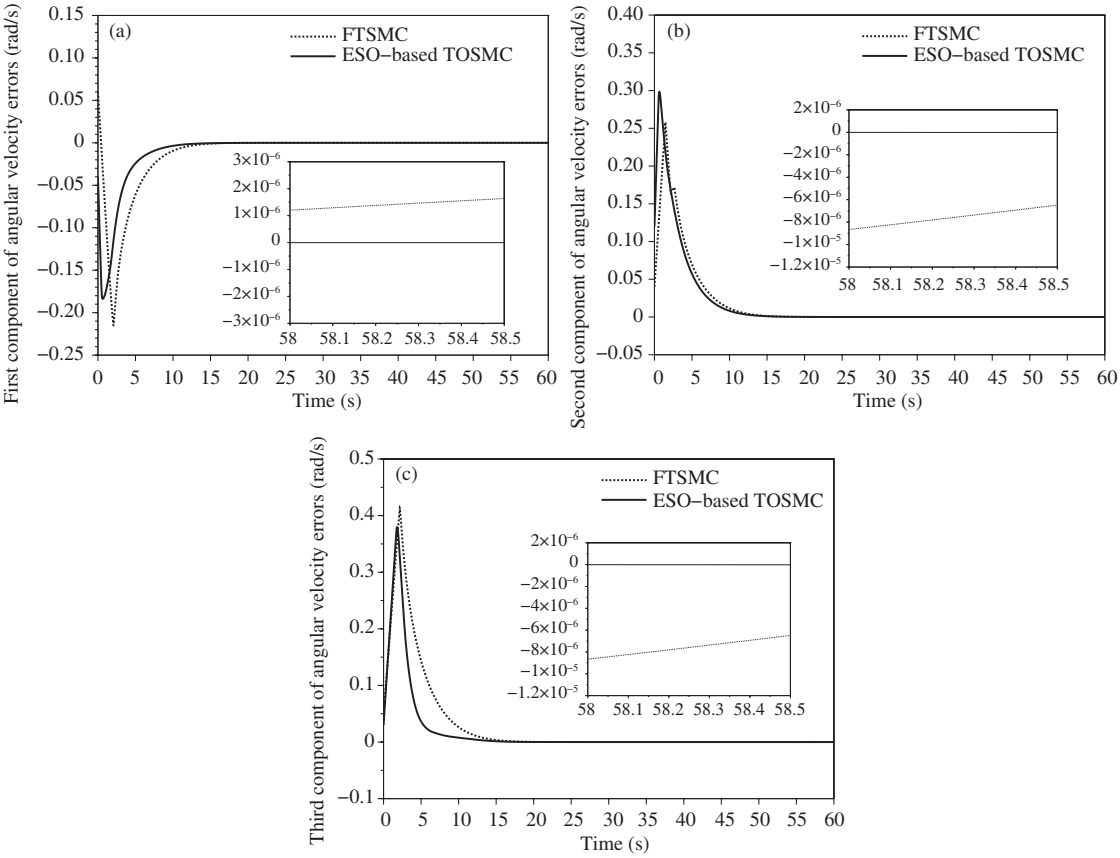

Figure 2 Angular velocity tracking error responses. The time history of (a) ω_{1e}, (b) ω_{2e}, (c) ω_{3e}.

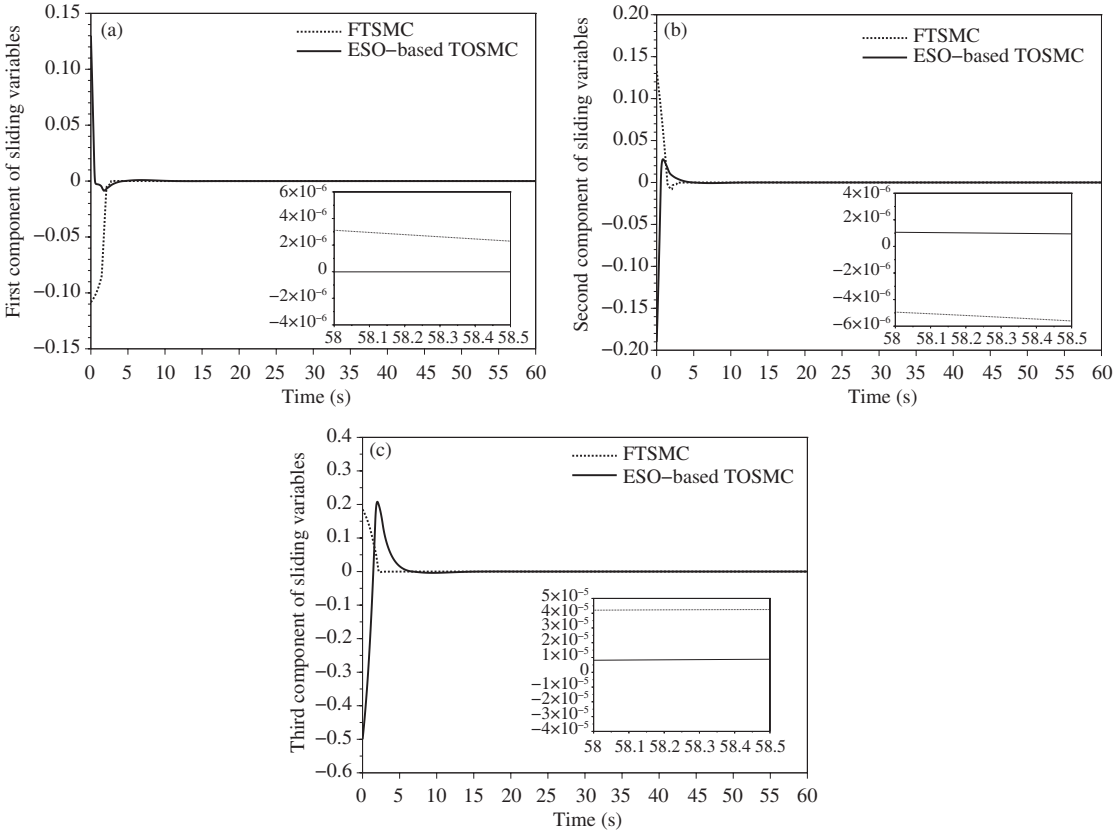

Figure 3 Sliding variables. The time history of (a) s_1, (b) s_2, (c) s_3.

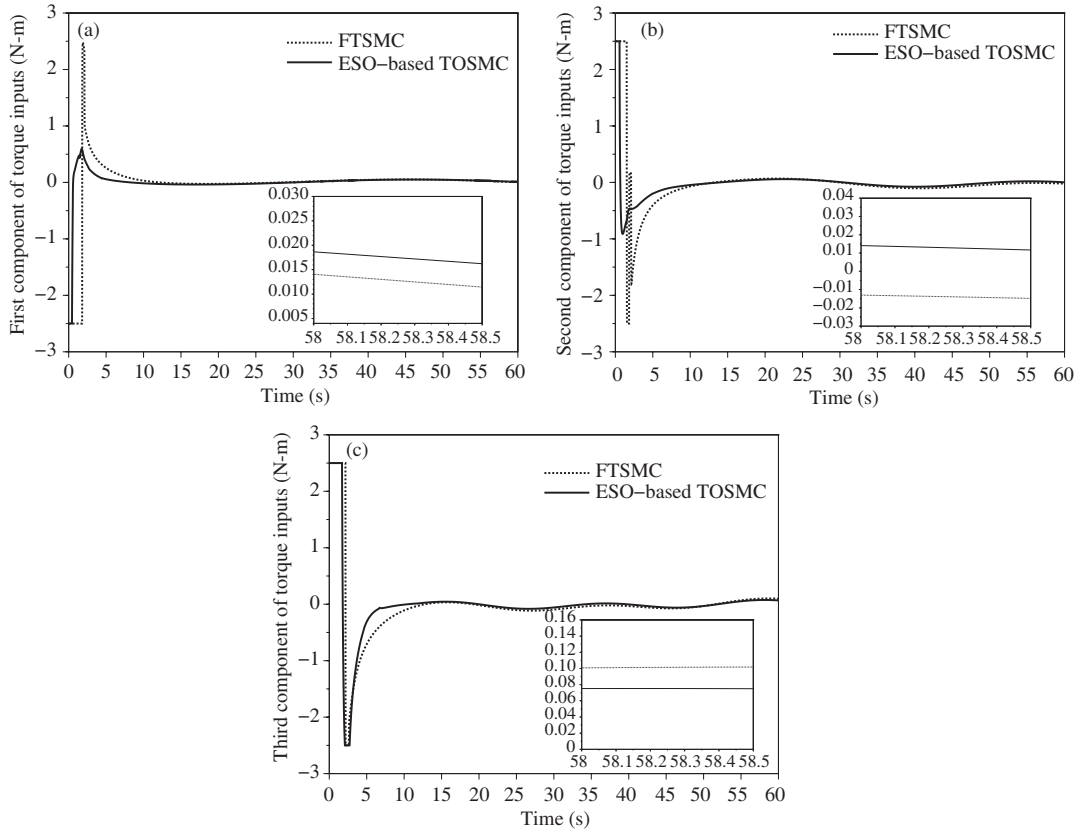

Figure 4 Control torque responses. The time history of (a) u_1, (b) u_2, (c) u_3.

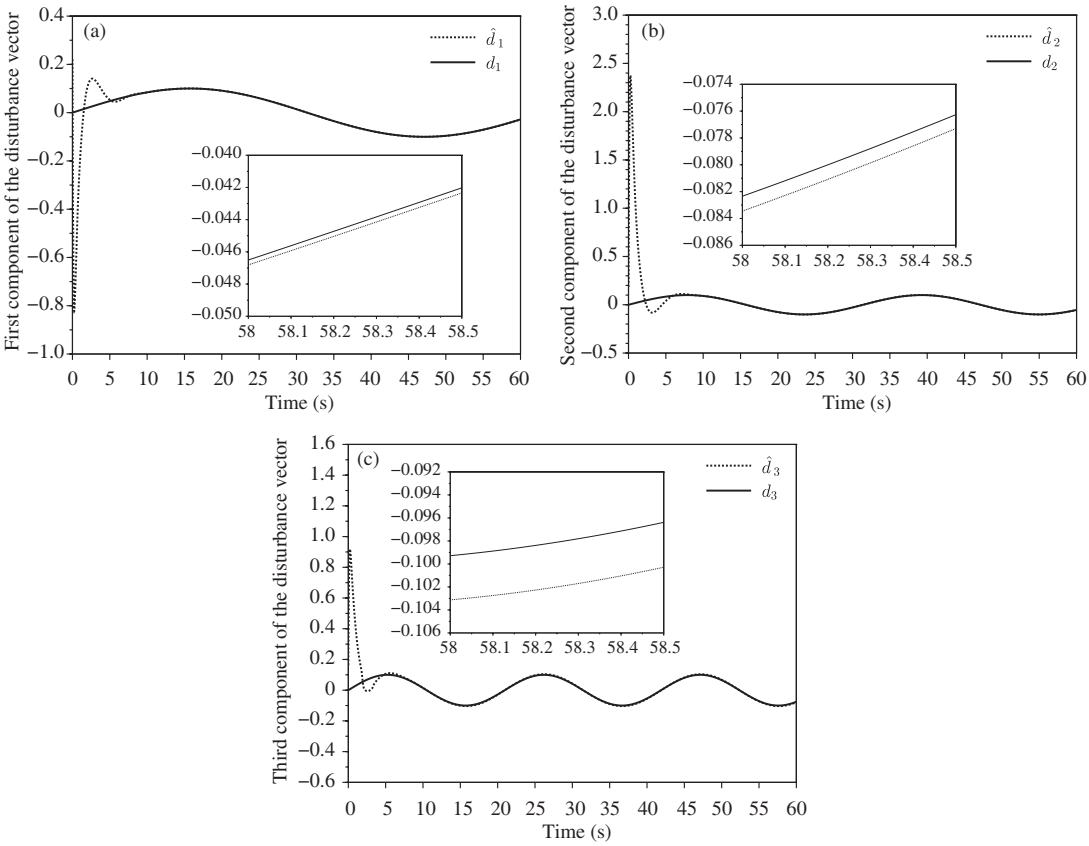

Figure 5 Estimated disturbance vector. The time history of (a) $\hat{d}_1$, (b) $\hat{d}_2$, (c) $\hat{d}_3$.

scheme is listed as $\|q_e\| \leqslant 5.56 \times 10^{-7}$, $\|\omega_e\| \leqslant 6.86 \times 10^{-7}$, and $\|s\| \leqslant 9.3 \times 10^{-7}$ with sampling time $h = 0.005$.

Evidently, the proposed control method achieves less variation of control signals and higher accuracy than the existing attitude controller. These simulation results verify the superiority of the designed controller for solving the attitude tracking control problem of a rigid spacecraft.

6 Conclusion

The ESO-based TOSMC scheme has been proposed for the attitude tracking control problem of a rigid spacecraft with inertia uncertainties, external disturbances and saturation input. First, a finite-time controller is designed based on TOSMC with nonsingular sliding surface to achieve precise accurate tracking responses and robust performance. This controller not only makes the attitude errors converge to the region containing the origin in finite time but also prevent the unwinding phenomenon. Then, a finite-time extended stated observer is constructed to estimate total disturbances of the system. The ESO-based TOSMC technique yields improved disturbance rejection and precise attitude tracking. The Lyapunov stability theory is employed to prove that the overall closed-loop system is finite-time stable. Numerical simulations on attitude control of a spacecraft model have been conducted to verify the effectiveness of the proposed controller.

Acknowledgements The work was supported by King Mongkut's University of Technology North Bangkok and Thailand Research Fund (TRF) (Grant No. RSA6080043).

References

1 Chen Z Y, Huang J. Attitude tracking and disturbance rejection of rigid spacecraft by adaptive control. IEEE Trans Autom Control, 2009, 54: 600–605
2 Zhu Z, Xia Y Q, Fu M Y. Adaptive sliding mode control for attitude stabilization with actuator saturation. IEEE Trans Ind Electron, 2011, 58: 4898–4907
3 Yeh F K. Sliding-mode adaptive attitude controller design for spacecrafts with thrusters. IET Control Theory Appl, 2010, 4: 1254–1264
4 Lu K F, Xia Y Q, Zhu Z, et al. Sliding mode attitude tracking of rigid spacecraft with disturbances. J Franklin Inst, 2012, 349: 413–440
5 Luo W C, Chu Y C, Ling K V. Inverse optimal adaptive control for attitude tracking of spacecraft. IEEE Trans Autom Control, 2005, 50: 1639–1654
6 Pukdeboon C, Zinober A S I. Control Lyapunov function optimal sliding mode controllers for attitude tracking of spacecraft. J Franklin Inst, 2012, 349: 456–475
7 Zou A M. Finite-time output feedback attitude tracking control for rigid spacecraft. IEEE Trans Control Syst Technol, 2014, 22: 338–345
8 Show L L, Juang J C, Jan Y W. An LMI-based nonlinear attitude control approach. IEEE Trans Control Syst Technol, 2003, 11: 73–83
9 Cong B L, Liu X D, Chen Z. Backstepping based adaptive sliding mode control for spacecraft attitude maneuvers. J Aerosp Eng, 2013, 22: 1–7
10 Guo Y, Song S M. Adaptive finite-time backstepping control for attitude tracking of spacecraft based on rotation matrix. Chinese J Aeronaut, 2014, 27: 375–382
11 Pisu P, Serrani A. Attitude tracking with adaptive rejection of rate gyro disturbances. IEEE Trans Autom Control, 2007, 52: 2374–2379
12 Zou A M, Kumar K D. Adaptive fuzzy fault-tolerant attitude control of spacecraft. Control Eng Pract, 2011, 19: 10–21
13 Utkin V I. Sliding Modes in Control and Optimization. Berlin: Spinger, 1992
14 Bhat S P, Bernstein D S. Finite-time stability of continuous autonomous systems. SIAM J Control Opt, 2000, 38: 751–766
15 Bhat S P, Bernstein D S. Geometric homogeneity with applications to finite-time stability. Math Control Signal Syst, 2005, 17: 101–127
16 Man Z H, Paplinski A P, Wu H R. A robust MIMO terminal sliding mode control scheme for rigid robotic manipulators. IEEE Trans Autom Control, 1994, 39: 2464–2469
17 Wu Y Q, Yu X H, Man Z H. Terminal sliding mode control design for uncertain dynamic systems. Syst Control Lett, 1998, 34: 281–287
18 Lu K F, Xia Y Q. Finite-time fault-tolerant control for rigid spacecraft with actuator saturations. IET Control Theory Appl, 2013, 7: 1529–1539
19 Pukdeboon C, Siricharuanun P. Nonsingular terminal sliding mode based finite-time control for spacecraft attitude tracking. Int J Control Autom Syst, 2014, 12: 530–540
20 Guo Y, Song S M, Li X H. Quaternion-based finite-time control for attitude tracking of the spacecraft without unwinding. Int J Control Autom Syst, 2015, 13: 1351–1359
21 Zhao L, Jia Y M. Finite-time attitude tracking control for a rigid spacecraft using time-varying terminal sliding mode techniques. Int J Control, 2015, 88: 1150–1162
22 Tiwari P M, Janardhanan S, un Nabi M. Rigid spacecraft attitude control using adaptive integral second order sliding mode. Aerosp Sci Technol, 2015, 42: 50–57
23 Gui H, Vukovich G. Adaptive integral sliding mode control for spacecraft attitude tracking with actuator uncertainty. J Franklin Inst, 2015, 352: 5832–5852
24 Chen M, Wu Q X, Cui R X. Terminal sliding mode tracking control for a class of SISO uncertain nonlinear systems. ISA Trans, 2013, 52: 198–206
25 Wallsgrove R J, Akella M R. Globally stabilizing saturated attitude control in the presence of bounded unknown disturbances. J Guid Control Dyn, 2005, 28: 957–963
26 Bošković J D, Li S M, Mehra R K. Robust adaptive variable structure control of spacecraft under control input saturation. J Guid Control Dyn, 2001, 24: 14–22
27 Hu Q L, Li B, Qi J T. Disturbance observer based finite-time attitude control for rigid spacecraft under input saturation. Aerosp Sci Technol, 2014, 39: 13–21
28 Laghrouche S, Smaoui M, Plestan F, et al. Higher order sliding mode control based on optimal approach of an electropneumatic actuator. Int J Control, 2006, 79: 119–131
29 Benahdouga S, Boukhetala D, Boudjema F. Decentralized high order sliding mode control of multimachine power systems. Int J Electr Power Energy Syst, 2012, 43: 1081–1086
30 Tian B L, Zong Q, Wang J, et al. Quasi-continuous high-order sliding mode controller design for reusable launch vehicles in reentry phase. Aerosp Sci Technol, 2013, 28: 198–207
31 Delprat S, de Loza A F. High order sliding mode control for hybrid vehicle stability. Int J Syst Sci, 2014, 45: 1202–1212
32 Perruquetti W, Barbot J P. Sliding Mode Control in Engineering. New York: Marcel Dekker, 2002
33 Edwards C, Colet E F, Fridman L. Advances in Variable Structure and Sliding Mode Control. Berlin: Springer, 2006
34 Levant A. Higher-order sliding modes, differentiation and output-feedback control. Int J Control, 2003, 76: 924–941

35 Levant A, Pridor A, Gitizadeh R, et al. Aircraft pitch control via second-order sliding technique. J Guid Control Dyn, 2000, 23: 586–594

36 Shtessel Y B, Shkolnikov I A, Levant A. Smooth second-order sliding modes: missile guidance application. Automatica, 2007, 43: 1470–1476

37 Pukdeboon C. Output feedback second order sliding mode control for spacecraft attitude and translation motion. Int J Control Autom Syst, 2016, 14: 411–424

38 Pukdeboon C, Zinober A S I, Thein M W L. Quasi-continuous higher order sliding-mode controllers for spacecraft-attitude-tracking maneuvers. IEEE Trans Ind Electron, 2010, 57: 1436–1444

39 Shen Y X, Shao K Y, Ren W J, et al. Diving control of autonomous underwater vehicle based on improved active disturbance rejection control approach. Neurocomputing, 2016, 173: 1377–1385

40 Su Y X, Zheng C H, Duan B Y. Automatic disturbances rejection controller for precise motion control of permanent-magnet synchronous motors. IEEE Trans Ind Electron, 2005, 52: 814–823

41 Zhu Z, Xu D, Liu J M, et al. Missile guidance law based on extended state observer. IEEE Trans Ind Electron, 2013, 60: 5882–5891

42 Lu K F, Xia Y Q. Finite-time fault-tolerant control for rigid spacecraft with actuator saturations. IET Control Theory Appl, 2013, 7: 1529–1539

43 Yang J, Li S H, Yu X H. Sliding-mode control for systems with mismatched uncertainties via a disturbance observer. IEEE Trans Ind Electron, 2012, 60: 160–169

44 Yang J, Li S H, Su J Y, et al. Continuous nonsingular terminal sliding mode control for systems with mismatched disturbances. Automatica, 2013, 49: 2287–2291

45 Yang J, Su J Y, Li S H, et al. High-order mismatched disturbance compensation for motion control systems via a continuous dynamic sliding-mode approach. IEEE Trans Ind Inf, 2014, 10: 604–614

46 Yang J, Chen W H, Li S H, et al. Disturbance/uncertainty estimation and attenuation techniques in PMSM drives — a survey. IEEE Trans Ind Electron, 2017, 64: 3273–3285

47 Wertz J R. Spacecraft Attitude Determination and Control. Berlin: Kluwer Academic, 1978

48 Sidi M J. Spacecraft Dynamics and Control a Practical Engineering Approach. Cambridge: Cambridge University Press, 1997

49 Shuster M D. A survey of attitude representations. J Astronaut Sci, 1993, 41: 439–517

50 Lan Q X, Qian C J, Li S H. Finite-time disturbance observer design and attitude tracking control of a rigid spacecraft. J Dyn Syst Meas Control, 2017, 139: 061010

51 Yan R D, Wu Z. Attitude stabilization of flexible spacecrafts via extended disturbance observer based controller. Acta Astronaut, 2017, 133: 73–80

52 Zhong C X, Chen Z Y, Guo Y. Attitude control for flexible spacecraft with disturbance rejection. IEEE Trans Aerosp Electron Syst, 2017, 53: 101–110

53 Chen M, Ren B B, Wu Q X, et al. Anti-disturbance control of hypersonic flight vehicles with input saturation using disturbance observer. Sci China Inf Sci, 2015, 58: 070202